

# Nanoscale

Accepted Manuscript



This is an *Accepted Manuscript*, which has been through the Royal Society of Chemistry peer review process and has been accepted for publication.

*Accepted Manuscripts* are published online shortly after acceptance, before technical editing, formatting and proof reading. Using this free service, authors can make their results available to the community, in citable form, before we publish the edited article. We will replace this *Accepted Manuscript* with the edited and formatted *Advance Article* as soon as it is available.

You can find more information about *Accepted Manuscripts* in the [Information for Authors](#).

Please note that technical editing may introduce minor changes to the text and/or graphics, which may alter content. The journal's standard [Terms & Conditions](#) and the [Ethical guidelines](#) still apply. In no event shall the Royal Society of Chemistry be held responsible for any errors or omissions in this *Accepted Manuscript* or any consequences arising from the use of any information it contains.

Cite this: 10.1002/sml.((please add manuscript number))

www.rsc.org/xxxxxx

## ARTICLE TYPE

# Graphene oxide immobilized enzymes show high thermal and solvent stability

Soňa Hermanová<sup>a</sup>, Marie Zarevucká<sup>b</sup>, Daniel Bouša<sup>c</sup>, Martin Pumera<sup>d</sup>, and Zdeněk Sofer<sup>\*c</sup>

Received (in XXX, XXX) Xth XXXXXXXXX 20XX, Accepted Xth XXXXXXXXX 20XX

DOI: 10.1002/b000000x

Thermal and solvent tolerance of the enzymes is of high importance for their industrial use. We show here that enzyme lipase from *Rhizopus oryzae* exhibit exceptionally high thermal stability and high solvent tolerance and even increased activity in acetone when immobilized onto graphene oxide (GO) nanosupport prepared by Staudenmaier and Brodie methods. We studied various forms of immobilization of enzyme, by physical adsorption, covalent attachment, and additional crosslinking. The activity recovery was shown to be dependent on the support type, enzyme loading and immobilization procedure. Covalently immobilized lipase showed significantly better resistance to heating inactivation (activity recovery 65 % at 70 °C) in comparison with soluble counterpart (activity recovery 65 % at 40 °C). Physically adsorbed lipase maintained even over 100 % of initial activity in a series of organic solvents. These findings, showing enhanced thermal stability and solvent tolerance of graphene oxide immobilized enzyme, will have profound impact on practical industrial scale uses of enzymes for conversion of lipids into the fuels.

## Introduction

The effective and highly selective catalysis by enzymes have led in the widespread use of enzymes in industrial processes<sup>1</sup>, biomedical assays<sup>2</sup> (ELISA<sup>3</sup>) and detection technologies.<sup>4</sup> One of the very important enzymes is lipase<sup>5</sup>, which is inexpensive biocatalyst capable of breaking down the lipids with very important applications in conversion of oil into the fuel.<sup>6</sup> One of the main challenges in the use of the enzymes is their stability; they often show drastic decrease of catalytic activity when exposed to increased temperature or organic solvents. Here we show that when the lipase is immobilized on graphene oxide, it is highly resistant to thermal and solvent exposure and it retains its activity at extreme conditions.

Graphene and graphene oxide (GO) has been studied as interesting nanosupport for a variety of biologically active agents leading to novel biocatalysts, biosensors, and drug delivery vehicles.<sup>7</sup> The morphology and large accessible surface area of GO nanosheets along with formation of stable aqueous suspension fulfill the criteria for high enzyme loading on support and thus for the development of catalysts for biotechnological applications.<sup>8</sup> Enzymes were immobilized on GO through covalent bonding due to the functional groups on the GO surface or by a cross-linker, and/or non-covalent binding through weak interactions. *I.e.* oxidoreductases, such as horse-radish peroxidase and oxalate oxidase were successfully immobilized on GO surface without any pretreatment and the extent of electrostatic interactions between enzyme and nanomaterial surface were proved to tune according to degree of GO's reduction.<sup>9,10</sup> The introduction of a glutaraldehyde spacer arm on the GO support enables tethering of enzyme molecules to yield bio-conjugates with improved thermostability, reusability and storage stability.<sup>11-</sup>

13

Herein, we investigated the effect of GOs prepared by two different routes (Brodie and Staudenmaier) as nanomaterial support for lipase. Lipase from *Rhizopus oryzae* (ROL) was studied as a model hydrolase for immobilization. Pentane-1,5-dial (glutaraldehyde) modification of GO support was applied along with cross-linking of enzyme previously adsorbed on GO and with coincident addition of enzyme and glutaraldehyde to GO. We will demonstrate that GO immobilized lipase shows thermal stability retaining up to 65 % activity at 70 °C if immobilized on GO, which is approx. 10-fold higher than for native, non-immobilized enzyme.

## Experimental

### Materials

All the reagents were of analytical grade. For the GO synthesis, sulfuric acid (98 %), nitric acid (98 %), potassium chlorate (98 %), hydrochloric acid (35 %), acetone (99.9 %) and isopropanol (99.9 %) were purchased from Penta, Czech Republic. Graphite (2 - 15 μm, 99.9995 %) was obtained from Alfa Aesar, Germany. Acetonitrile (p.a.) was purchased from Sigma-Aldrich, Czech Republic. Toluene (p.a.) and n-hexane (p.a.) were supplied by Lach-Ner, Czech Republic. All solvents were dried with molecular sieves before use. Glutaraldehyde (25 % v/v in water), p-nitrophenyl laurate (pNPL) and lipase from *Rhizopus oryzae* (no. 62305), activity 2.96 U/mg were supplied by Sigma-Aldrich, Czech Republic and used as received.

Two types of graphene oxide: BR GO and ST GO with BET surface area of 4.3 m<sup>2</sup>/g and of 6.6 m<sup>2</sup>/g, respectively, and differing in the surface chemistry and surface charge were studied

as immobilization supports. The synthesis of Brodie graphene oxide and Staudenmaier graphene oxide was performed according to procedures reported previously.<sup>14,15</sup> The nanomaterial properties are reported in detail by Pumera et al.<sup>16,17</sup>

## Synthetic procedures

### Enzyme activity assay

Lipolytic activity of free and immobilized enzymes was determined on UV/VIS HELLIOS spectrophotometer (DELTA Thermospectronic, England) by measuring the absorbance at 420 nm produced by the released p-nitrophenol in the hydrolysis of pNPL. The reaction mixture consisted of 0.125 ml free or immobilized lipase suspension, 1.625 ml of phosphate buffer (56 mM, pH 7) and 0.125 ml of 2.5 mM pNPL (in ethanol). Hydrolytic reaction was carried out at 25 °C for 30 min under continuous stirring and afterwards, 0.25 ml of 0.1 M Na<sub>2</sub>CO<sub>3</sub> was added to stop the reaction. The activity was measured three times and average value and standard deviation were determined.

One unit of lipase activity (U) was defined as the amount of enzyme that caused the release of 1 μmol of p-nitrophenol from pNPL in 1 min under the test conditions.

### Enzyme immobilization

Graphene oxide (GO) dispersion, prepared by adding 5 mg of GO to 3 ml of phosphate buffer (56 mM, pH 7.0), was stirred for 15 min, ultrasonicated for 60 min and then used for immobilization procedure. Non-covalent enzyme immobilization in phosphate buffer solution (56 mM, pH 7.0) was performed according to the reported procedure.<sup>12</sup> For procedures including covalent attachment, glutaraldehyde (0.9 ml, 25 % v/v in water) was added as follows:

- i) to GO dispersion (3 ml) before immobilization
- ii) to non-specifically immobilized enzyme on GO (3 ml)
- iii) to GO dispersion (3 ml) coincidentally with 1 ml of enzyme solution (0.5 mg/ml).

Immobilized enzymes were separated by centrifugation, washed three times with phosphate buffer (56 mM, pH 7.0) and stored at 4 °C. The experiments were carried out three times and the standard deviation was up to 9 %. The immobilization efficiency was evaluated in terms of enzyme immobilization yield and activity recovery expressed in percentage as follows:

$$\text{Immobilization yield} = \frac{\text{amount of coupled proteins}}{\text{amount of introduced proteins}} * 100$$

$$\text{Activity recovery} = \frac{\text{immobilized lipase activity}}{\text{free lipase activity}} * 100$$

The amount of protein content was determined by the method of Bradford using bovine serum albumin as the standard.<sup>24</sup>

### Thermal stability assay

The thermal stability assays were performed by pre-incubation of immobilized ROL in phosphate buffer (56 mM, pH 7.0) at various temperatures (30 - 70 °C) for 1 h, followed by measurement of the residual enzyme activity at 25 °C as described above.

### Optimum pH evaluation

The effect of pH on the activity of the free and immobilized lipase enzyme was studied at 25 °C in various buffers in the pH range varying from 5 to 10 using pNPL as a substrate. Buffers used were 50 mM acetate (pH 5), 50 mM citrate-phosphate (pH 6.0), 50 mM phosphate (pH 7.0), 50 mM Tris-HCl (pH 8.0 - 9.0),

50 mM glycine-NaOH (pH 10.0).

### Stability in organic solvents

The dispersion of immobilized lipases was filtered; pellets were washed by acetone and dried at 37 °C for 24 h. Immobilized enzyme (1 mg) was incubated with 1 ml of solvents at 25 °C for 1 h. Subsequently, the solvent was removed by filtration. Retained solid phase (immobilized ROL) was washed two times with 2 ml of acetone and by 1 ml of phosphate buffer (0.56 M, pH 7.0), centrifuged at 5,000 rpm, and finally the supernatant was decanted. Residual lipase activity was measured as above mentioned. Biocatalyst not exposed to the organic solvent was used as the reference.

## Methods

Combustible elemental analysis (CHNS-O) was performed with a PE 2400 Series II CHNS/O Analyzer (Perkin Elmer, USA). In CHN operating mode (the most robust and interference free mode), the instrument employs a classical combustion principle to convert the sample elements to simple gases (CO<sub>2</sub>, H<sub>2</sub>O and N<sub>2</sub>). The PE 2400 analyzer performs combustion, reduction, homogenization of product gases, separation and detection automatically. A microbalance MX5 (Mettler Toledo) is used for precise weighing of samples (1.5 - 2.5 mg per single sample analysis). The accuracy of CHN determination is better than 0.30 % abs. Internal calibration is performed using N-fenyl urea.

FTIR spectra were collected on FTIR spectrometer Nicolet 6700 (Thermo Scientific, USA) equipped with a diamond crystal GladiATR (PIKE Technologies, USA). The GO samples were placed at the surface of the diamond crystal and were pressed with a press tip flap system. The samples were scanned in the wavenumbers range of 4000 - 400 cm<sup>-1</sup> and corrected against the background spectrum of air. The spectrum of each sample was obtained by taking the average of 64 scans. Diamond ATR crystal and DTGS detector were used for the measurements. Binomial 11 points smoothing of the spectrum was applied.

*inVia* Raman microscope (Renishaw, England) was used for Raman spectroscopy in backscattering geometry with CCD detector and DPSS laser (532 nm, 5 mW) with 50x magnification objective. Instrument calibration was achieved with a silicon reference which gives a peak position at 520 cm<sup>-1</sup> and a resolution of less than 1 cm<sup>-1</sup>. Samples used for the measurement were dispersed in isopropanol (1 mg/ml) and dried on silicon wafer.

High resolution X-ray photoelectron spectroscopy (XPS) was performed with a ESCAProbeP (Omicron Nanotechnology Ltd, Germany) spectrometer using a monochromatic aluminum X-ray radiation source (1486.7 eV). The freshly cut indium block homogeneously covered with graphene was used for the measurement. Al X-ray source with a monochromator was applied for the excitation.

The zeta potential of the GO and immobilized ROL was measured by the Zetasizer Nano ZS (Malvern, England) in phosphate buffer (56 mM, pH 7.0). Laser doppler microelectrophoresis using interferometric technique was used for the measurement.

## Results and discussion

Graphene oxides were prepared by chlorate based methods, Brodie and Staudenmaier. These methods are based on oxidation of graphite by potassium perchlorate in fuming nitric acid for Brodie method (termed as BR GO)<sup>14</sup> and the mixture of fuming

nitric acid and sulphuric acid for Staudenmaier method (termed as ST GO)<sup>15</sup>, respectively. Combustion elemental analysis proved the different composition of carbon, oxygen, and hydrogen for both types of supports (Table 1 and Table SI 1). The C/O ratio, calculated according to the C 1s and O 1s peak area, is 5.3 for ST GO and only 1.3 for BR GO. Lower C/O ratio indicates higher concentration of hydrophilic oxygen functional group on BR GO in comparison with ST GO.

This fact is documented by high resolution XPS spectra of C 1s peak provided in Table 2. The deconvolution of C1s peak was performed in order to resolve different valence state of carbon (see Figure 1, 2). The data show main peak associated with C=C and C-C bond located around 284.5 eV and 285.5 eV, respectively. Asymmetric tail related to oxygen functional groups (like C-O, C=O and O-C=O) is located in the range of 286 - 290 eV. High asymmetric tail of BR-GO sample indicates high concentration of oxygen functional groups. The presence of large amount of hydrophobic sp<sup>2</sup> hybridized carbon atoms in ST GO is documented by high resolution C 1s peak spectra, where significantly lower concentration of oxygen functionalities is observed.

In addition, the Raman and IR spectroscopy analysis of BR GO and ST GO sample was performed (Figure 3). High luminescence background of BR GO indicates high concentration of oxygen functional groups. According to FTIR analysis epoxy groups were also detected on BR GO, which was documented by peak located at 950 cm<sup>-1</sup>. The concentration of carboxylic groups (about 0.22 wt. % for BR GO and 1.18 wt. % for ST GO measured by alkalimetric titration with 0.1 M NaOH) was found out very low in comparison with other types of GOs which use permanganate based oxidation methods.

For one type of covalent immobilization both types of GOs were treated by bifunctional agent-glutaraldehyde to introduce electrophilic functional groups on the surface. The glutaraldehyde modified GOs were characterized by ATR-FTIR spectroscopy and the spectra with absorption bands ascribed to C-H stretching are depicted in Figure 4a.<sup>18,19</sup> In ideal case one aldehyde group of glutaraldehyde is assumed to react with GO's hydroxyl group to form the hemiacetal structure and the pendant one is available for the reaction with primary amine groups of protein molecules during their covalent attachment to the support.

In the case of direct enzyme adsorption onto GO, hydrophobic interactions are suggested to dominate as lipases strongly adsorb to hydrophobic surfaces maintaining functional protein conformation.<sup>12</sup> The successful loading of enzyme protein onto GO supports was evidenced by FTIR spectroscopy (Figure 4b).

All immobilization procedures were performed in phosphate buffer solution at pH 7.0 and laboratory temperature. Under these conditions both GOs supports possessed negative charges as documented by zeta potentials values (Table 3). During following enzyme immobilization onto the support's surface the drop in absolute value of zeta potential, which was slightly pronounced for BR GO, implies that the carboxylic groups are involved in the interactions between enzyme molecules and GO's functional surface.<sup>9</sup>

Lipase ROL was directly immobilized onto both BR GO and ST GO supports without any chemical modification at neutral pH in phosphate buffer (56 mM). Incubation time of one hour was proved as optimal to reach maximum yields and no leaching occurred since both enzyme concentration and activity remain the same within a week.

The highest immobilization yield was attained at low ROL concentrations (100 - 500 µg/ml), where ST GO displayed higher adsorption capacity than BR GO (Figure 5 a, b). With increasing

soluble ROL concentration (7.5 - 15.0 mg/ml) a significant drop in immobilization yield was observed and the values were the same for both studied supports. Activity recovery dramatically decreased with increasing ROL concentration (Table 4), which could be consequence of protein-protein interactions taking place at high enzyme loading.<sup>20</sup> This is also supported by identical immobilization efficiency achieved independently of a studied support at soluble ROL concentration range of 7.5 - 15.0 mg/ml. The results imply stronger hydrophobic interactions between ROL and ST GO in comparison with BR GO, where non-specific electrostatic interactions are suggested to occur in higher extent, however under non-saturation conditions.

**Table 1** Elemental analysis of graphene oxide supports.

Sample	At.% N	At. % C	At. % S	At. % H	At. % O
BR GO	0.32	62.58	0.00	15.05	22.05
ST GO	0.25	70.47	0.00	11.34	17.94

**Table 2** The results of C 1s peak deconvolution show presence of various oxygen functional groups.

Functional group	BR GO %	ST GO %
C=C (284.5 eV)	2.7	55.2
C-C (285.4 eV)	24.5	9.6
C-O (286.6 eV)	24.4	14.6
C=O (287.6 eV)	45.8	8.1
O-C=O (289.8 eV)	1.9	5.2
$\pi$ - $\pi$ * interaction (291.0 eV)	0.7	7.4

In all covalent immobilization procedures, where glutaraldehyde chemistry was involved, the quantitative immobilization yield was obtained under conditions optimal for direct immobilization. Complete immobilization was accompanied with a large loss of native enzyme activity, which is a trend frequently reported in the literature.<sup>12,21</sup>

The thermal stability of ROL was studied within the temperature range of 30 - 70 °C and the results are shown in Figure 6a, b. The relative activity of free ROL decreased significantly above 40 °C and it retained only 23 % of its initial activity at 50 °C. All immobilization procedures resulted in enhanced thermal stability of ROL, which means an increase in the resistance of immobilized enzyme towards heating-induced conformational changes. The activity of ROL immobilized directly on BR GO decreased more slowly than that of ROL on ST GO at the temperature range from 40 °C to 50 °C, which reflects a contribution of stronger interactions than physical ones.

Significant increase in thermal stability of all covalently immobilized ROL is ascribed to covalent attachment. The glutaraldehyde treatment enables the formation of covalent bonds either intermolecular (cross-linking with glutaraldehyde) or covalent attachment to the glutaraldehyde-modified support.

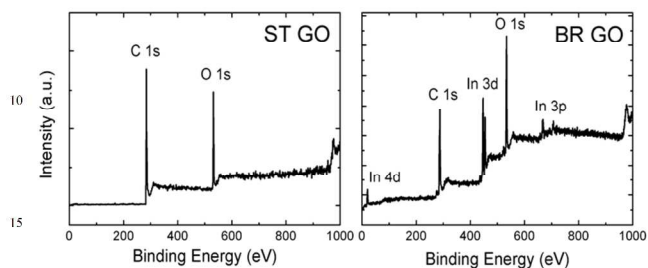


**Fig. 1** The XPS survey spectra of BR GO and ST GO samples.

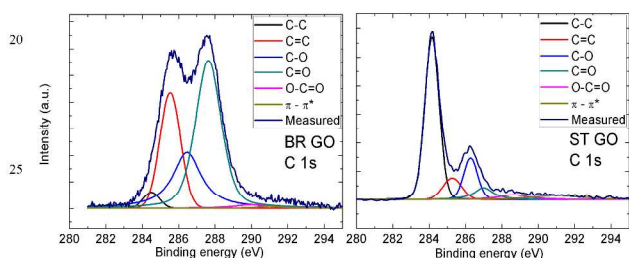


**Fig. 2** The high resolution XPS spectra of C 1s peak for BR GO and ST GO sample. Fittings of the individual C1s spectra shows the possible carbon bonds present in the graphene oxide.

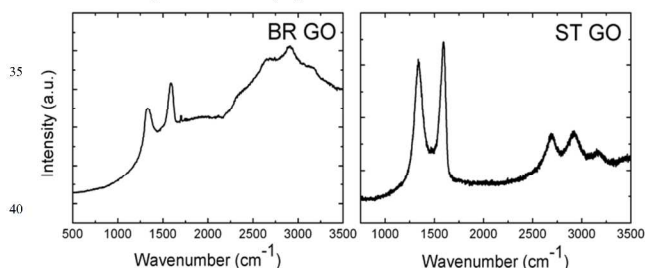


**Fig. 3** Raman spectra of graphene oxides. High background of BR GO sample is related to strong luminescence of graphene oxide.

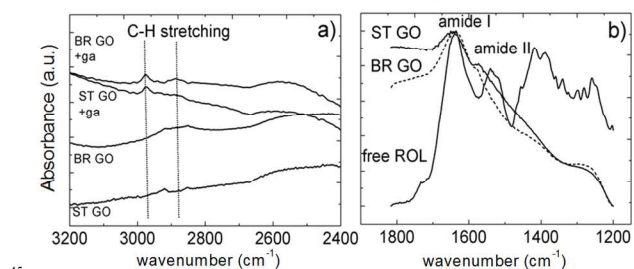


**Fig. 4** Selected region of FTIR spectra of glutaraldehyde (ga) modified ST GO and BR GO (a), amide bands region of free ROL and ROL immobilized directly on BR GO and ST GO (b).

Consequently enzyme un-folding was restricted or the rigidification of enzyme structure by multipoint covalent linkage occurred.<sup>22</sup> Free lipase retained only 6 % of its initial activity after incubation at 70 °C as compared to 65 % activity retention of the immobilized lipase at the same conditions. Such enhanced thermal stability would improve the catalytic performance of immobilized enzyme in the organic synthesis as at higher temperatures the reaction rates are significantly enhanced and the reaction affords high yields.<sup>23</sup>

**Table 3** Comparison of the surface charge via zeta potential measurement of GO supports and immobilized ROL in phosphate buffer (56 mM, pH 7.0).

Sample	Zeta potential / FWHM of charge distribution in mV	
	BR GO	ST GO
GO	-34.0/12.8	-27.2/16.1
GO modified by glutaraldehyde	-31.6/12.4	-26.2/9.7
Direct immobilization	-11.5/13.4	-11.2/12.9
ROL + GO modified by glutaraldehyde	-13.4/18.0	-16.0/14.3
ROL + GO followed by crosslinking by glutaraldehyde	-15.1/18.6	-15.9/13.9
ROL immobilized on GO in the presence of glutaraldehyde	-16.2/14.6	-15.1/18.6

**Table 4** Activity recovery of ROI on BR GO and ST GO supports using glutaraldehyde chemistry (concentration of soluble ROL 100 µg/ml).

Immobilization system	Activity recovery %	
	BR GO	ST GO
ROL + GO modified by glutaraldehyde	8.4	16.3
Cross-linked ROL + GO	3.4	4.5
ROL immobilized on GO in the presence of glutaraldehyde	7.5	14.9

<sup>a</sup>) standard deviation was  $\leq 0.5$  %

The pH optima of free and selected immobilized ROL are depicted in Figure 7. Free ROL showed a broad pH optimum in the range of 7.0 - 9.0. Directly immobilized ROL on both supports had pH optimum at 8.0 and displayed improved pH stability in the acidic region. Assuming the pH dependent properties of GO's support itself, in acidic medium carboxylic groups at the edges are protonated and the hydrophobic character of the GO sheets is increased. Consequently there is a lower proton concentration in the microenvironment of physically adsorbed enzyme than in bulk solution, which correlates well with measured pH profile. With increasing solution alkalinity carboxylic and also phenolic groups localized at GOs' surface undergo deprotonation<sup>24</sup>, which increases electrostatic repulsion between the sheets. Consequently, the increase in negative charge and its density on the support surface could negatively influence the immobilized enzyme orientation and hence cause a loss in activity (see Figure SI 1).

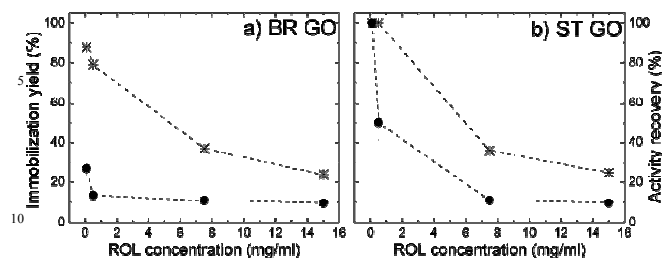


Fig. 5 Dependence of immobilization yield (star) and activity recovery (circle) of ROL directly immobilized on BR GO (a), and ST GO (b) on soluble ROL concentration used for immobilization.

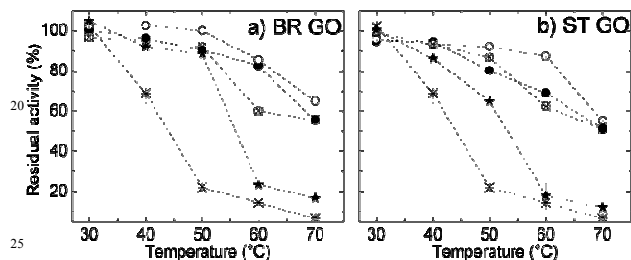


Fig. 6 Thermal stability of ROL immobilized on BR GO (a) and ST GO (b): free ROL (star), directly immobilized ROL (solid star), ROL covalently immobilized on glutaraldehyde modified GO (empty circle), cross-linked ROL on GO (solid circle), coincident addition of glutaraldehyde and ROL to GO (crossed circle).

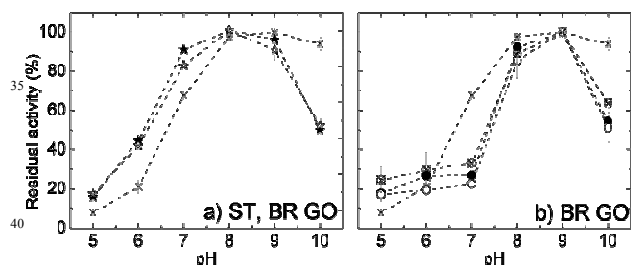


Fig. 7 pH optimum of ROL directly immobilized on BR GO and ST GO (a), and ROL covalently immobilized on BR GO (b): free ROL (star), directly immobilized ROL (solid star), ROL covalently immobilized on glutaraldehyde modified GO (empty circle), cross-linked ROL on GO (solid circle), coincident addition of glutaraldehyde and ROL to GO (crossed circle).

The pH activity profiles of all covalently immobilized ROLs on both GO supports displayed almost identical behavior. The curves possessed a narrower bell shape with a maximum at pH 9.0. Independent of the support or covalent immobilization protocol the immobilized ROLs showed higher sensitivity towards alkaline (above 9.0) or acidic regions in comparison with soluble enzyme. However, under acidic conditions some activity loss could be connected with enzyme leaching as Schiff's bases become unstable and convert back to the aldehyde and amine.

Kinetic parameters of free and immobilized enzyme were determined by measurement of ROL activity for hydrolysis of p-NPL substrate with various concentrations (1.75 to 5.00 mM) in phosphate buffer. The interaction of substrate itself and GOs was not considered under study conditions since the hydrolysis reaction did not proceed in the absence of ROL. Almost for all immobilized ROL a decrease in apparent  $K_m$  value was observed indicating higher affinity to enzyme-substrate complex formation (Table 5).

Table 5 Kinetics parameters of soluble and immobilized ROL on ST GO and BR GO supports determined for the hydrolysis of pNPL at 25 °C and pH 7.0.

Sample	$K_m$	$V_{max}$	$K_m$	$V_{max}$
	[mM]	[U/mg]	[mM]	[U/mg]
	BR GO		ST GO	
Direct immobilization	0.30	0.17	0.11	0.14
GO modified by glutaraldehyde+ RO	0.29	0.05	0.22	0.04
Cross-linked RO +GO	1.63	0.07	0.11	0.01
RO immobilized on GO in the presence of glutaraldehyde	0.06	0.02	0.09	0.02

\* Soluble ROL:  $K_m = 0.44$  mM,  $V_{max} = 2.60$  U/mg

The  $V_{max}$  values indicates the maximum reaction rate, when all the enzyme sites are saturated with substrate. Both physically adsorbed ROL on ST GO and BR GO exhibited 19-fold and 15-fold, respectively, drop in  $V_{max}$  value in comparison to soluble enzyme. The decrease was even lower for all immobilized ROL prepared by covalent immobilization as the consequence of multiple bond linkages which, in turns positively increased the thermal stability of immobilized enzyme. The decrease in  $V_{max}$  could be ascribed to lower substrate concentration in the microenvironment of the immobilized lipase, which is caused by diffusion limitations. The same trend for kinetics parameters of the free and lipase immobilized on activated carbon support has been reported in literature.<sup>20,25</sup> Sharp increase in  $K_m$  observed for cross-linked ROL immobilized on BR GO ( $K_m = 1.63$ ) indicated undesirable decrease in its affinity for substrate molecules. The results could be ascribed to partial inactivation of active centers.

The effect of several organic solvents on the stability of immobilized ROL, which displayed highest activity recovery (ROL on ST GO) and storage stability (ROL covalently bound on glutaraldehyde modified ST GO) was determined. The following organic solvents were selected and classified according to their values of Log P and dipole moment, respectively: acetonitrile (-0.33, 3.2), acetone (-0.23, 2.88), isopropanol (0.28, 1.66), toluene (2.5, 0.36) and n-hexane (3.5, 0). Attempts to establish a correlation with either log P or dipole moment were not successful. Valivety et al. stated that there is probably no single parameter for solvent polarity according which the enzyme activity in organic solvent would be predicted.<sup>26</sup>

Hydrolytic activity of the ROL on ST GO in non-polar solvents (toluene, n-hexane) after incubation was 109 % compared to that of the control without solvent (100 %). This behaviour can be attributed to the fact that non-polar organic solvents do not strip off the water layer from the surface of enzyme. Interestingly, relative activity retention of ROL covalently immobilized on modified ST GO was low (31 % and 18 %) after the incubation in toluene and n-hexane, respectively. These results show that it is not possible to establish a general rule on the immobilized enzyme behaviour regarding activity and stability in non-polar solvents. Although, the instability of lipases in aprotic polar solvents was frequently observed causing by the stripping of water from the protein surface, along with solvent penetration into the enzyme, leading to protein unfolding and subsequent denaturation.<sup>27</sup> The highest activity recovery of both tested immobilized lipases was found after their incubation in

acetone (Table 6). Our findings are supported by several reports describing the stability of lipases in aprotic polar solvents. A lipase produced by *Pseudomonas* sp. had activity coupling from 100 to 110 % in acetone, tetrahydrofuran and ethyl acetate.<sup>27</sup> Lipase from *Mucor javanicus* exhibited high stability and an increased activity in acetonitrile, ethyl acetate and acetone as well.<sup>28</sup> Given that lipase's catalytic performance is dependent on their tolerance to different solvent systems the finding that our lipase showed significantly high stability in acetone (activity recovery of 221.4±2.1 %) and isopropanol (158.4±7.8 %) suggests its potential as a biocatalyst for transesterification reaction and biodiesel production.

**Table 6** Activity recovery of ROL on ST GO support.

Solvent	Activity recovery in %	
	Direct immobilization ROL on ST GO	ST GO modified by glutaraldehyde+ ROL
acetonitrile	107.4±2.4	4.6±0.5
acetone	221.4±2.1	58.9±2.4
control	100.0±0	100.0±0
isopropanol	158.4±7.8	6.1±0.9
toluene	109.7±1	31.8±3.4
n-hexane	109.9±2.7	18.1±1.2

## 15 Conclusion

We have demonstrated that lipase immobilized on graphene oxide retains its activity at high temperature (85 % of its initial activity at 60 °C and 65 % of activity at 70 °C) when compared to native, non-immobilized enzyme (~65 % activity recovery at 40 °C). This has very profound implication to the use of this enzyme for fuel production. The study confirmed successful immobilization of lipase with potential synthesis application onto graphene oxide supports. The tunable presence and distribution of hydrophobic domains in concert with surrounding hydrophilic groups on the graphene oxide surface makes it advantageous carrier for straightforward and efficient lipase binding. Lipase adsorption accompanied with minor unspecific interactions contributed to the stabilization of active protein conformation "open lid" like, which was consequently maintained in organic solvent. From the viewpoint of activity retention, number of immobilization procedure steps, costs of reagents, etc. physical adsorption was proved as the optimal procedure. The pH and thermal stability of both immobilized lipase preparations was also enhanced (ROL directly immobilized on ST GO, BR GO). Generally, the incubation in organic solvents increased activity of ROL adsorbed on ST GO, which suggests that directly immobilized biocatalysts have great potential in biotechnological processes. In particular, the produced biocatalyst ROL on ST GO shows potential with polar solvents, which have technological advantages such as low toxicity, low boiling points, low costs and the possibility to use polar substrates for novel reactions.

## Acknowledgements

Z.S., D.B. and S.H. were supported by Specific University Research grant (MSMT 20/2015) and Czech science foundation (project no. 15-09001S). M.Z. thanks the Academy of Science of the Czech Republic (project No. M200551203) for financial support. M.P. acknowledges Tier 2 grant (MOE2013-T2-1-056) from Ministry of Education, Singapore. Authors acknowledge Dr. Stanislava Voběrková for valuable technical assistance during lab work.

## Notes and references

- <sup>a</sup>Department of Polymers, University of Chemistry and Technology Prague, Technická 5, 166 28 Prague 6, Czech Republic  
E-mail: sona.heranova@vscht.cz
- <sup>b</sup>Institute of Organic Chemistry and Biochemistry ASCR, Flemingovo nám. 2, 166 10 Prague 6, Czech Republic  
E-mail: zarevucka@uochb.cas.cz
- <sup>c</sup>Department of Inorganic Chemistry, University of Chemistry and Technology Prague, Technická 5, 166 28 Prague 6, Czech Republic  
E-mail: zdenek.sofer@vscht.cz
- <sup>d</sup>Division of Chemistry & Biological Chemistry, School of Physical and Mathematical Sciences, Nanyang Technological University, 21 Nanyang Link, Singapore 637371, Singapore, E-mail: pumera@ntu.edu.sg

† Footnotes should appear here. These might include comments relevant to but not central to the matter under discussion, limited experimental and spectral data, and crystallographic data.

<sup>70</sup> Electronic Supplementary Information (ESI) available: [details of any supplementary information available should be included here]. See DOI: 10.1039/b000000x/

- R. DiCosimo, J. McAuliffe, A. J. Poulou, G. Bohlmann, *Chem. Soc. Rev.* 2013, **42**, 6437.
- Z. Wang, P. Huang, A. Bhirde, A. Jin, Y. Ma, G. Niu, N. Neamati, X. Chen, *Chem. Commun.* 2012, **48**, 9768.
- R. Hnasko, A. Lin, J. A. McGarvey, L. H. Stanker, *Biochem. Biophys. Res. Commun.* 2011, **410**, 726.
- A. Amine, H. Mohammadi, I. Bourais, G. Palleschi, *Biosens. Bioelectron.* 2006, **21**, 1405.
- D. Sharma, B. Sharma, A. K. Shukla, *Biotechnology.* 2011, **10**, 23-40.
- G. Chen, M. Ying, W. Li, *Appl. Biochem. Biotechnol.* 2006, **911**, 129-132.
- T. Kuila, S. Bose, P. Khanra, A. K. Mishra, N. H. Kim, J. H. Lee, *Biosens. Bioelectron.* 2011, **26**, 4637.
- F. Zhao, H. Li, Y. Jiang, X. Wang, X. Mu, *Green Chem.* 2014, **16**, 2558.
- J. Zhang, F. Zhang, H. Yang, X. Huang, H. Liu, J. Zhang, S. Guo, *Langmuir* 2010, **26**, 6083.
- Y. Zhang, J. Zhang, X. Huang, X. Zhou, H. Wu, S. Guo, *Small* 2012, **8**, 154.
- R. Su, P. Shi, M. Zhu, F. Hong, D. Li, *Bioresour. Technol.* 2012, **115**, 136.
- I. V. Pavlidis, T. Vorhaben, T. Tsoufis, P. Rudolf, U. T. Bornscheuer, D. Gournis, H. Stamatidis, *Bioresour. Technol.* 2012, **115**, 164-171.
- D. Kishore, M. Talat, O. N. Srivastava, A. M. Kayastha, *PLoS ONE* 2012, **7**, e40708.
- B. C. Brodie, *Phil. Trans. R. Soc. Lond.* 1859, **149**, 249.
- L. Staudenmaier, *Berichte der Deutschen Chemischen Gesellschaft* 1898, **31**, 1481.
- C. K. Chua, Z. Sofer, M. Pumera, *Chem. Eur. J.* 2012, **18**, 13453.
- H. L. Poh, F. Sanek, A. Ambrosi, G. Zhao, Z. Sofer, M. Pumera, *Nanoscale* 2012, **4**, 3515.
- P. Podsiadlo, A. K. Kaushik, E. M. Arruda, A. M. Waas, B. S. Shim, J. Xu, H. Nandivada, B. G. Pumplun, J. Lahann, A. Ramamoorthy, N. A. Kotov, *Science* 2007, **318**, 80.
- H. Nantao, M. Lei, G. Rungang, W. Yanyan, C. Jing, Y. Zhi, K. Eric Siu-Wai, Z. Yafei, *Nano-Micro Lett.* 2011, **3**, 215.
- K. Ramani, R. Boopathy, C. Vidya, L. J. Kennedy, M. Velan, G. Sekaran, *Process Biochem.* 2010, **45**, 986.
- J. T. Cang-Rong, G. Pastorin, *Nanotechnology* 2009, **20**, 255102.

- 
22. C. Mateo, J. M. Palomo, G. Fernandez-Lorente, J. M. Guisan, R. Fernandez-Lafuente, *Enzyme Microb. Technol.* 2007, **40**, 1451.
  23. L. Fjerbaek, K. V. Christensen, B. Norddahl, *Biotechnol. Bioeng.* 2009, **102**, 1298.
  - 5 24. B. Konkana, S. Vasudevan, *J. Phys. Chem. Lett.* 2012, **3**, 867.
  25. L. John Kennedy, P. K. Selvi, P. Aruna, K. N. Hema, G. Sekaran, *Chemosphere* 2007, **69**, 262.
  - 26 R. H. Valivety, G. A. Johnston, C. J. Suckling, P. J. Halling, *Biotechnol. Bioeng.* 1991, **38**, 1137.
  - 10 27. M. Pogorevc, H. Stecher, K. Faber, *Biotechnol. Lett.* 2002, **24**, 857.
  28. J. C. Wu, S. S. Lee, M. M. B. Mahmood, Y. Chow, M. M. R. Talukder, W. J. Choi, *J. Mol. Catal. B: Enzym.* 2007, **45**, 108.